AGU PUBLICATIONS

Geophysical Research Letters

RESEARCH LETTER
10.1002/2015GL065602

Key Points:
- Many locations have non-Gaussian temperature distributions
- Some locations have short warm-side tails
- Places with short tails may experience a large increase in warm extremes

Supporting Information:
- Text S1 and Figures S1 and S5
- Figure S1
- Figure S2
- Figure S3
- Figure S4
- Figure S5

Correspondence to:
P. C. Loikith,
ploikith@pdx.edu

Citation:
Loikith, P. C., and J. D. Neelin (2015), Short-tailed temperature distributions over North America and implications for future changes in extremes, *Geophys. Res. Lett.*, *42*, 8577–8585, doi:10.1002/2015GL065602.

Received 30 JUL 2015
Accepted 9 SEP 2015
Accepted article online 5 OCT 2015
Published online 23 OCT 2015

Short-tailed temperature distributions over North America and implications for future changes in extremes

Paul C. Loikith[1,2] and J. David Neelin[3]

[1]Department of Geography, Portland State University, Portland, Oregon, USA, [2]Jet Propulsion Laboratory, California Institute of Technology, Pasadena, California, USA, [3]Department of Atmospheric and Oceanic Sciences, University of California Los Angeles, Los Angeles, California, USA

Abstract Some regions of North America exhibit nonnormal temperature distributions. Shorter-than-Gaussian warm tails are a special subset of these cases, with potentially meaningful implications for future changes in extreme warm temperatures under anthropogenic global warming. Locations exhibiting shorter-than-Gaussian warm tails would experience a greater increase in extreme warm temperature exceedances than a location with a Gaussian or long warm-side tail under a simple uniform warm shift in the distribution. Here we identify regions exhibiting such behavior over North America and demonstrate the effect of a simple warm shift on changes in extreme warm temperature exceedances. Some locations exceed the 95th percentile of the original distribution by greater than 40% of the time after this uniform shift. While the manner in which distributions change under global warming may be more complex than a simple shift, these results provide an observational baseline for climate model evaluation.

1. Introduction

Global warming is often presented in terms of changes in mean temperature; however, changes in extremes are likely to have the most severe impact on the environment and society [*Seneviratne et al*., 2012]. Several recent observational studies present evidence of changes in temperature extremes over the past several decades [*Donat et al*., 2013; *Fischer and Knutti*, 2014; *Perkins et al*., 2012] with attribution of these changes largely due to anthropogenic forcing [*Christidis*, 2005; *Morak et al*., 2013]. Overall, observed changes have been relatively similar in magnitude for the cold and warm tails of the temperature probability distribution function (PDF), with some exceptions [*Morak et al*., 2013]. For example, warming of the cold tail is greater in magnitude than warming of the warm tail in regions experiencing snow and ice retreat [*Kharin et al*., 2007]. Future changes in temperature extremes are anticipated to be much greater than those observed with large increases in the number of extreme warm events and large decreases in the number of extreme cold events [*Coumou and Robinson*, 2013; *Kharin et al*., 2013; *Kirtman et al*., 2013; *Zwiers et al*., 2011]. Such changes would expose vulnerable populations to unprecedented heat extremes [*Meehl et al*., 2009; *Rowe and Derry*, 2012; *Sillmann et al*., 2013].

PDFs of daily 2 m temperature (T2m) exhibit marked departures from Gaussianity in the tails over much of North America (NA). Using station data, *Cavanaugh and Shen* [2014] documented the first four statistical moments of the temperature PDF, finding large and coherent regions of non-Gaussian distributions. *Perron and Sura* [2013] identified regions of non-Gaussian temperature PDFs in global reanalysis and *Loikith et al*. [2013] documented wintertime skewness of T2m in reanalysis over NA. *Stefanova et al*. [2013] showed that the non-Gaussianity of higher moments of the temperature PDF using station data over the southeastern United States (U.S.) is modulated by large-scale modes of climate variability such as the El Niño–Southern Oscillation, signifying an important role of large-scale atmospheric circulation in the shape of the PDF.

As skewness relates to PDF symmetry and the relative length of the distribution tails, changes in skewness would result in asymmetrical changes in temperature extremes. While such changes have been suggested, they are rarely statistically significant to date. *Donat and Alexander* [2012] showed positive, but not significant, trends in skewness of gridded annual daily temperature over northern NA. *Cavanaugh and Shen* [2014] showed statistically significant trends in temperature skewness over NA at some observation stations. *Rhines and Huybers* [2013] and *Weaver et al*. [2014] demonstrated that observed changes in extremes are

primarily due to changes in mean temperature and not higher moments at the global scale. *Huntingford et al*. [2013] further suggest a lack of change in global temperature variability concurrent with observed warming. *Lau and Nath* [2012] showed that increases in extreme warm temperatures over portions of NA as projected by a high-resolution global climate model are largely a result of a shift in the mean and not a result of changes at higher moments. *Huybers et al*. [2014] suggested, however, that in the case of nonnormal distributions, warming is unlikely to result in a simple distribution shift due to nonlinear interactions between the mean and tails. In this case, a purely uniform warming may be implausible at some locations.

It can be expected that advective processes play an important role in the shape of daily temperature PDFs. Non-Gaussian, approximately exponential, PDF tails are common for several passive tropospheric chemical tracers and water vapor [*Neelin et al*., 2010], consistent with expectations from simple mathematical prototypes for passive tracer advection problems with a forcing that maintains a gradient [e.g., *Bourlioux and Majda,* 2002; *Majda and Gershgorin*, 2010]. This tracer advection paradigm illustrates the relationship between the structure of distribution tails and physical mechanisms and suggests tail sensitivity in other variables influenced by advective processes such as T2m. Highlighting implications of non-Gaussian PDFs for future changes in extreme events, *Ruff and Neelin* [2012] presented several examples of locations with longer-than-Gaussian temperature PDF tails using station data. They demonstrated that under the simple scenario of a uniform warming across the PDF, a location with a long warm tail would experience a relatively smaller increase in extreme warm temperature exceedances than a location with a Gaussian tail. This implies that locations with shorter-than-Gaussian warm-side tails would experience a greater increase in warm temperature exceedances under a simple rightward shift than locations with a Gaussian distribution resulting in potentially large impacts.

Whether surface temperature warming is to be primarily manifested as a shift, or whether the shape of non-Gaussian tails may change, the tails of the present-day daily temperature PDF can play a leading role in indicating how locations will be affected by a warming climate. Recognizing that warming could be realized in multiple ways, this paper demonstrates the effect of the simplest case, a uniform shift across the distribution and how extreme warm temperature exceedances are impacted at locations with shorter-than-Gaussian warm-side distribution tails. Furthermore, it is shown that considering the physically motivated case of a shift leads to variants of tests for non-Gaussianity that can be useful for evaluating tails in present-day distributions.

2. Data and Methodology

Daily mean T2m data are computed from the *Wang and Zeng* [2014a, 2014b] suite of global land, hourly data sets [*Wang and Zeng*, 2013]. Here we use the product combining NASA's Modern Era Retrospective-Analysis for Research and Applications reanalysis [*Rienecker et al*. [2011]] with the Climate Research Unit 3.10 [*Mitchell and Jones,* 2005] gridded monthly T2m observations. While this product has inherent uncertainties originating largely from the reanalysis, it has been validated in recent studies [*Loikith et al*., 2015a; *Loikith et al*., 2015b; *Wang and Zeng*, 2013; *Wang and Zeng*, 2014a, 2014b; *Wang and Zeng*, 2015]. Additional validation is presented in Figures S1 and S2 in the supporting information. All analysis is performed on anomalies, computed by removing the daily climatology from each day then removing the linear trend. Results are presented for winter and summer defined as December-January-February (DJF) and June-July-August (JJA), respectively. Temperature distributions are computed by binning daily T2m every 1.0°C (0.5°C) for DJF (JJA) with the smaller bin width for JJA used because of the generally lower daily temperature variance in summer versus winter. Bin counts are normalized by the maximum count.

For reference, a Gaussian curve is presented for each example. *Ruff and Neelin* [2012] used the core of the distribution, defined as all bins exceeding 0.3 of the distribution maximum, to compute the Gaussian fit using polynomial regression. This reduces the influence non-Gaussian tails have on the standard deviation (σ) of the distribution. However, in some cases, non-Gaussian behavior within the core can result in a large σ when estimated in this manner. To avoid such cases, the Gaussian is fit to the core using the σ of the entire distribution if that value is smaller than the σ estimated from only the core. The 95th percentile of the temperature distribution is used to define threshold exceedances. A percentile threshold is chosen over a σ threshold so that all cases, regardless of Gaussianity, have the same frequency of exceedance days in the base climate. Distribution shifts are demonstrated using a 1σ warming so that all locations experience a similar warming

relative to variance (i.e., a 2°C warming is relatively small for a location with a σ of 12°C while it is a very large warming for a location with a σ of 4°C). In addition to this physically based reason, this choice proves highly useful for assessing statistical significance (see section 3c).

3. Examples of Short Tails and Shift-Induced Exceedances

3.1. Winter

Examples of DJF observed short warm-side tails, spanning a range of NA, are shown in Figure 1 with a postulated 1σ warm shift and corresponding Gaussian curves (solid lines). For reference, the grid cell locations are plotted in Figure 3. By definition, P95 is exceeded 5% of the time in the unshifted case. Below each PDF panel is a plot of the percentage of days exceeding the P95 of the unshifted distribution as a function of shift in σ. For reference, under the same 1σ warm shift, a Gaussian distribution would exceed its unshifted P95 by 26%.

The British Columbia example in Figure 1a exhibits a notably short warm tail, with the P95 far to the left of the range of Gaussian P95s. The effect of a 1σ warm shift is large at this location, with a temperature that is only exceeded 5% of the time in the unshifted distribution being exceeded nearly half of the time after the shift while a Gaussian would only exceed the preshifted P95 26% of the time. Here temperature variance is large so that a 1σ shift equates to a 5.9°C warming; however, Figure 1c shows that the effect is similar for a range of warmings. For example, a 0.5σ warming (~3°C) results in exceedance frequency greater than 20%, while for a Gaussian a 0.5σ shift would only result in an increase in exceedances of ~5%.

Similar behavior is seen in Figure 1b where the percentage of days that exceed P95 increases to 46% due to a 1σ warming. For the Great Plains example, 1σ is even greater than for the British Columbia example; however, Figure 1d shows that regardless of the shift magnitude, the observed distribution shows a much greater increase in exceedance frequency than the corresponding Gaussian.

Similar effects are found in drastically different climates as exemplified by the Florida and Yucatan examples in Figures 1e and 1f. For Florida, due to smaller variance, a 1σ shift equates to a 4°C warming which results in a 46% occurrence of exceeding the unshifted P95. In the Yucatan example, a relatively small 2.2°C warm shift would result in 43% of days exceeding the unshifted P95. As evident in Figure 1h, here a modest 1°C warming would still result in an increase in threshold exceedances of nearly 15%.

3.2. Summer

Overall, short warm-side tails in JJA tend to not deviate from Gaussian as much as in DJF; however because this is the warm season, the effect of increased exceedances has implications for heat waves and consequently human health. The coastal Louisiana example (Figure 2a) shows a large increase in exceedances (+32%) due to a very small warm shift of 1.6°C. In other words, a 1.6°C rightward shift in the distribution would result in an event that rarely occurs in the current climate to occur one third of the time. Conversely, if the distribution were Gaussian, that threshold would only be exceeded about one quarter of the time. Similar results are found in the Ohio Valley example in Figure 2b. The Great Basin and Arctic examples in Figure 2e and 2f, respectively, show less notable short tails, with the P95 of the unshifted distribution lying only slighting to the left of the Gaussian envelop in both cases. However, a 1σ shift still results in exceedance frequencies notably larger than the 26% expected from a Gaussian.

3.3. Measures of Statistical Significance in Departures From Gaussian

The shift of the present-day distribution and the change in exceedances of P95 described above in terms of practical implications has an important dual role as a test for non-Gaussianity. As elaborated in the SI, these yield variants of the Kolmogorov-Smirnov/Lilliefors (KS/L hereafter) test for normality [*Sheskin*, 2003]. Like KS/L, each is based on the cumulative density function (CDF), but using measures that have a straightforward physical interpretation is particularly relevant to the case of a warm-side short tail and reduces potential influence of a long cold side tail. Under these measures, the CDF of the observed time series is compared with a large ensemble of CDFs sampled from a comparable Gaussian.

Three measures are presented, based on the physically motivated question of how days exceeding a threshold temperature T_t change under a shift of the distribution. The first two are seen in the example PDFs of Figures 1 and 2, which motivate the choice seen in the maps in Figures 3 and 4. First, choosing T_t to be a given

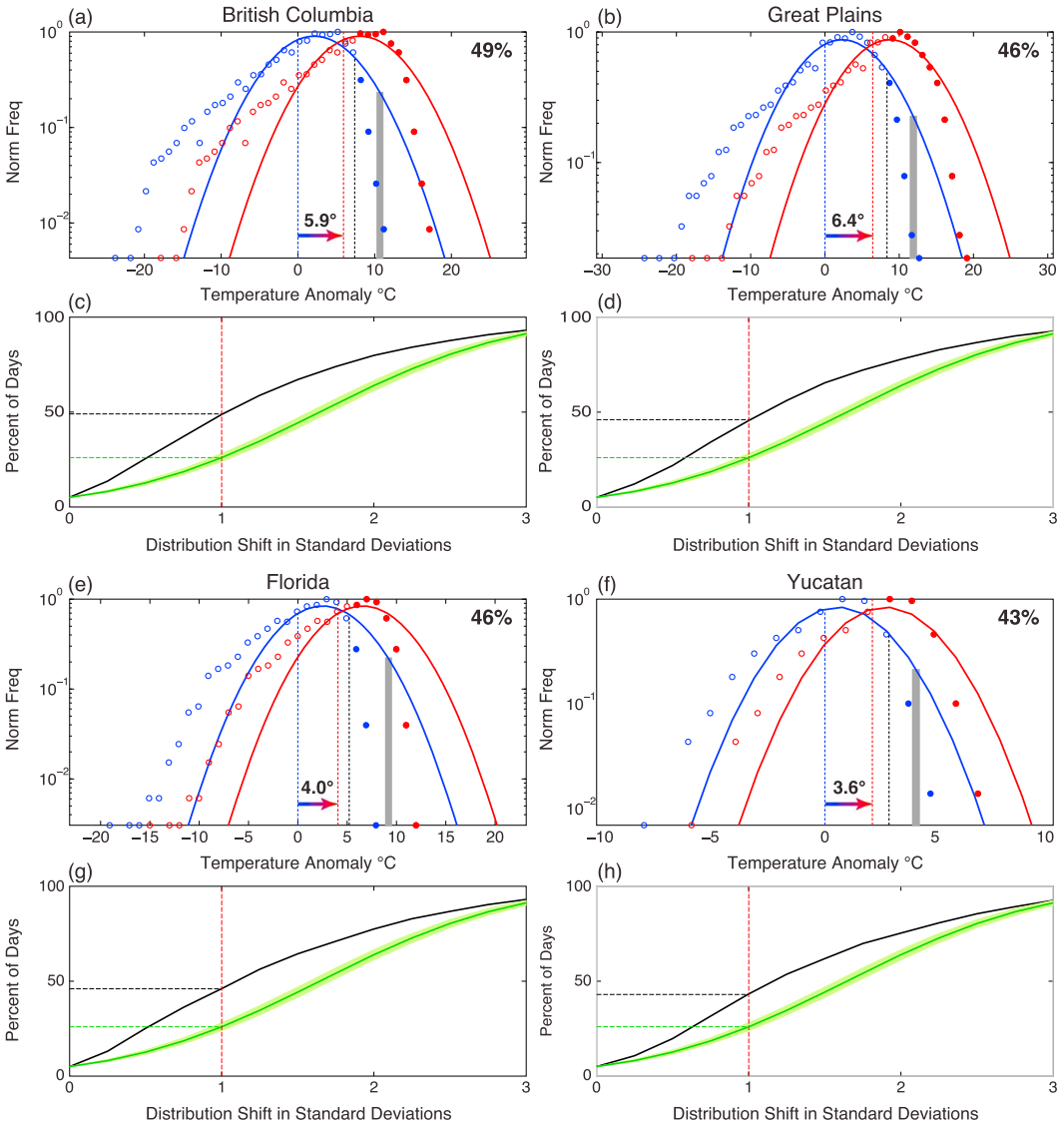

Figure 1. DJF temperature anomaly frequency distribution for DJF at the (a) British Columbia, (b) Great Plains, (e) Florida, and (f) Yucatan grid points. Locations of each grid point are shown in Figure 3. Bin counts (circles, 1°C width) are normalized by the maximum count and plotted on a log scale. Blue (red) circles are the preshifted (shifted) distributions after a uniform 1σ warming with filled (open) circles indicating bins above (below) the 95th percentile. The blue and red vertical lines indicate the mean of the preshifted distribution and the shifted distribution, respectively. The solid blue and red curves are Gaussian fits to the cores of the preshifted and postshifted distributions, respectively. The vertical black line is the preshifted 95th percentile. The shaded gray region is the 5th to 95th percentile range of 95th percentile temperature values determined by randomly sampling a Gaussian distribution with the same mean and standard deviation as the Gaussian fit to the observed distribution (solid blue). The 1σ shift in degrees is shown above the arrow, and the percentage of days exceeding the observed 95th percentile after the shift is noted on the top right. (c, d, g, h) Plots, corresponding to the distributions above each panel, of the percentage of days exceeding the observed 95th percentile of the distribution versus the magnitude of the shift in σ. Green curves are the median Gaussian values obtained from randomly sampling the Gaussian distribution and the 5th and 95th percentiles of this sample bound the shaded region. Black curves are for the observed distribution. Vertical red lines highlight a 1σ warm shift as in the above cases, and the black (green) horizontal line highlights the percent of days exceeding the preshifted 95th percentile due to a 1σ warm shift for the observed (Gaussian) cases. This value is always 26% for the Gaussian.

percentile, here P95, and measuring the separation of T_t between the empirical and reference CDF gives a statistic at a location in T_s chosen to be relevant to the warm tail (see Figures S3 and S4 for the relation to the KS/L statistic). Second, the fraction of days exceeding T_t as the distribution is shifted compared to that of the sampled reference distribution—chosen for its climate implications—is also a variant of the KS/L

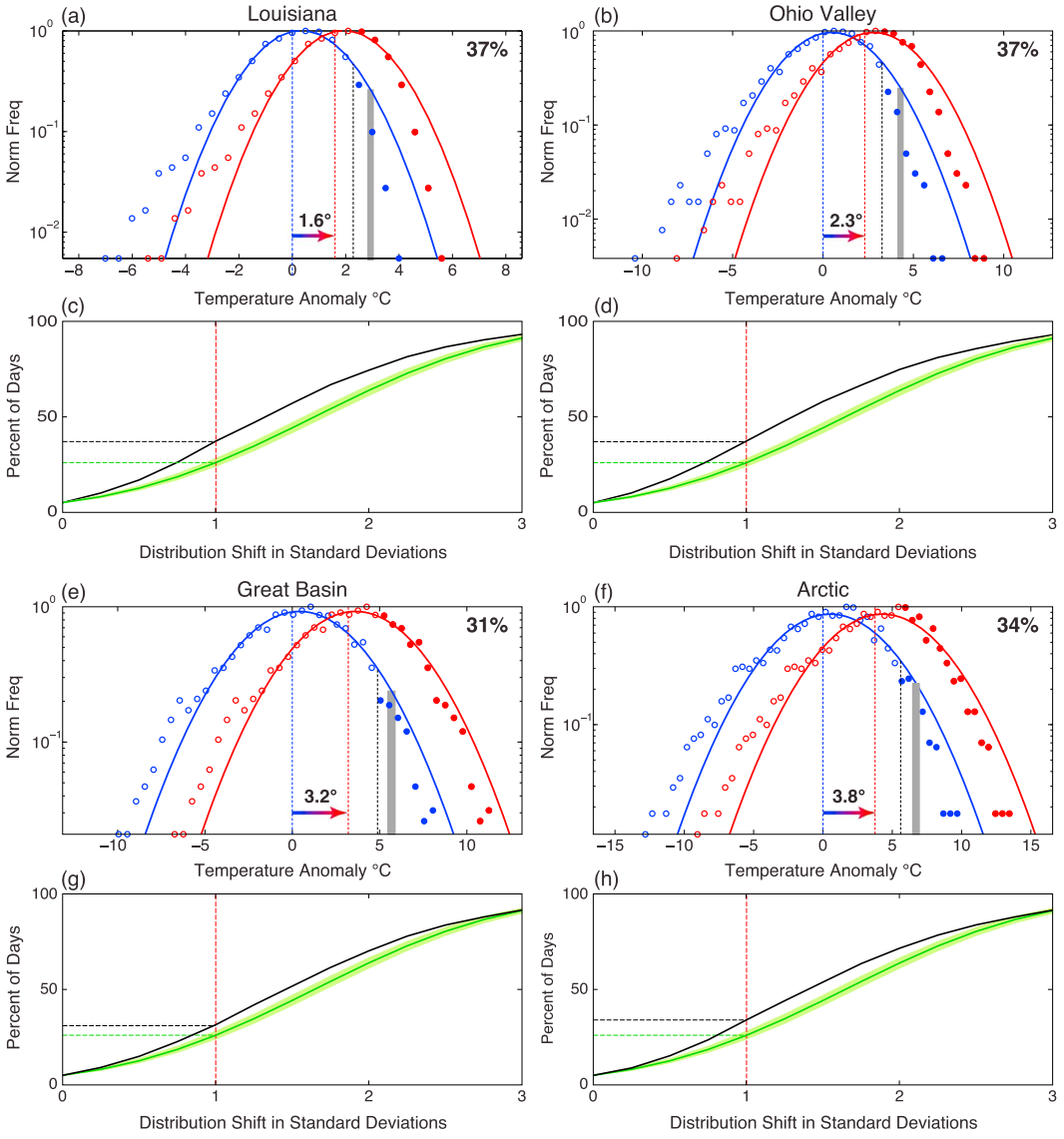

Figure 2. Same as in Figure 1 except for JJA and different locations.

procedure. To see this, note that the shift examined in sections 2a and 2b is equivalent to using the CDF of the shift variable $s = (T_t - T)/\sigma$. If the empirical CDF emerges from the envelope sampled from the reference Gaussian, the two differ at the specified level. Importantly, for this application, it is apparent when the differences in the slope that lead to this separation result from differences in PDF near T_t, the neighborhood of interest in the warm-side tail (as opposed to differences from Gaussian arising in the cold-side tail). Third, this leads to an index of non-Gaussianity from which maps can be plotted. Choosing the separation between these CDFs at a specific shift value, here $s = \sigma$, and comparing to the distribution sampled from the reference Gaussian creates a statistic that has a physical interpretation (increase in the fraction of days exceeding the threshold for the given shift relative to that of the Gaussian) and also has a direct relationship to a significance level.

4. Domain-Wide Exceedances

Expanding on the examples in section 3, Figures 3a and 4a show maps of the threshold exceedances for all grid cells when a uniform 1σ warming is applied to the PDF as in the above examples (similar patterns occur with a 0.5σ shift; see Figure S5). The map of σ is shown on the right of each figure for reference. Unshaded

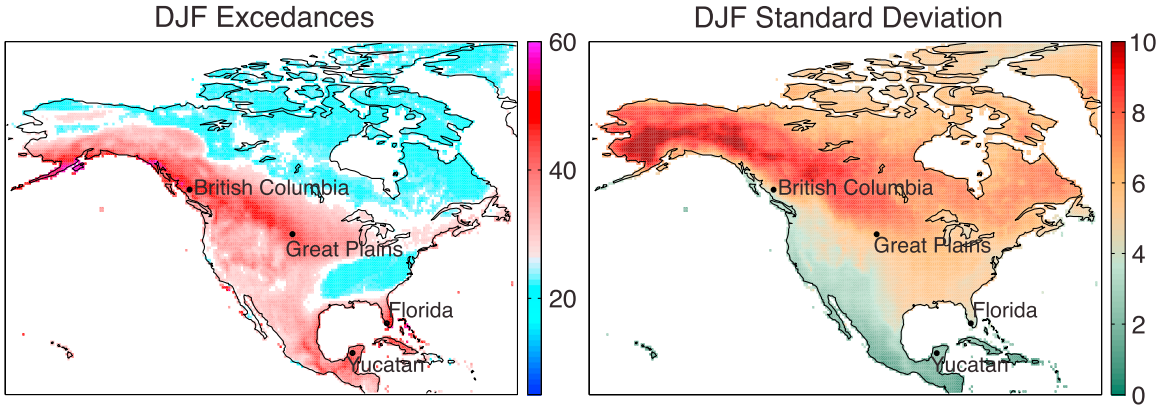

Figure 3. (left) Percentage of days exceeding the 95th percentile of the current temperature distribution after a 1σ warm shift. The location of the grid points used in the examples in Figure 1 is indicated by the labeled black dots. Red and blue shades respond to longer-than and shorter-than Gaussian tails, respectively. Regions with no shading are where the increase in threshold exceedances is not outside the 5th–95th percentile interval of random samples from a Gaussian distribution. The 1st–99th percentile range is 23–29 about the Gaussian value of 26. (right) Map of standard deviation for DJF temperature anomalies for each grid cell.

values less than 24% or greater than 28% are outside the 5th–95th percentile range determined by randomly sampling the reference Gaussian. In DJF (Figure 3), the most striking coherent region of relatively high threshold exceedances is along the Pacific Coast of Alaska and British Columbia stretching inland across the U.S.-Canada border and into the northern Great Plains including the British Columbia and Great Plains examples shown in Figure 1. In some coastal locations in Alaska, a temperature that is exceeded 5% of the time in the current climate would be exceeded nearly 60% under a 1σ warm shift. High values are also found throughout eastern and southern Mexico, Florida, and parts of the Caribbean, including the Florida and Yucatan examples shown in Figure 1. Relatively low increases in the frequency of threshold exceedances are found in the northern third of the domain and across the central and southeast U.S., associated with long warm tails in these regions (PDFs not shown). While we emphasize that a uniform shift may not be the most plausible global warming scenario at all locations, the large exceedances speak to the level of statistically significant non-Gaussianity and the prevalence of short warm-side tails.

In JJA (Figure 4), relatively large increases in threshold exceedances are found along the northern tier of Alaska and the Yukon and Northwest Territories, the Intermountain West of the U.S., the Midwest and mid-Atlantic of the U.S., and along the immediate Gulf of Mexico Coast. The implications for future temperature extremes are significant in these regions, with portions of the eastern half of the U.S. experiencing warm temperature extremes that only occur 5% of the time in the current climate up to 40% of the time in a climate with a 1σ shift. Such shifts are exemplified by the Ohio Valley and Louisiana cases shown in Figure 2.

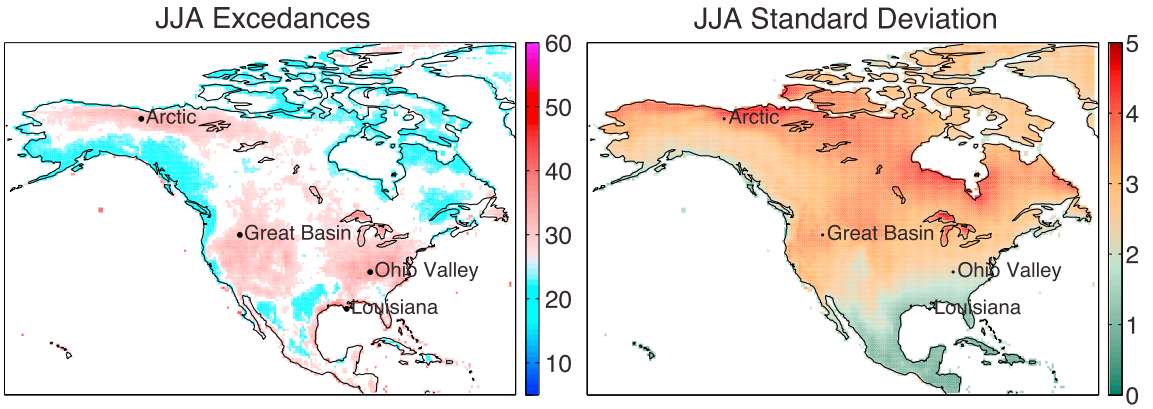

Figure 4. Same as in Figure 3 except for JJA.

5. Discussion and Conclusions

5.1. Meteorological Interpretation

This analysis shows that short warm-side tails occur in coherent regions at different spatial scales and across diverse geographic regions (e.g., coastal, inland, high, and low latitudes). We postulate, based on prior work [*Loikith and Broccoli*, 2012; *Loikith et al*., 2015a], that reasonable meteorological interpretations can be offered for these short tails. While this is a major undertaking, here we offer some examples of important factors.

Advection across a maintained gradient can yield short tails when the gradient is smaller on the warm side. For example, in DJF along the North Pacific coast, large excursions on the warm side of the PDF are limited by the moderating influence of the adjacent Pacific Ocean. The only source of relatively warm air during the winter is from the south, and any warm horizontal temperature advection would be substantially diminished through sensible cooling as the airmass travels over the relatively cool ocean.

In JJA, explanations are likely less linked to large-scale dynamics and more related to local limitations on warm-side excursions or processes related to land-atmosphere coupling or mesoscale circulation. For example, large excursions on the warm side of the PDF are likely limited along the coast of the Gulf of Mexico, the subtropical and tropical Pacific Ocean, and the Caribbean Sea relative to inland areas because of the moderating influence of sea breezes. Over the mountains of the western U.S., short warm tails could be related to summertime convection. The way in which temperature warms for a given location in the future will be influenced by how these mechanisms change, providing a target for physics and process-based model analysis of future climate projections.

5.2. Summary and Conclusions

Non-Gaussian temperature distributions are common throughout NA, with several regions exhibiting shorter-than-Gaussian warm-side distribution tails. In such cases, a uniform warm shift in the distribution results in larger increases in extreme warm threshold exceedances than if the distribution was Gaussian. This paper identifies several examples of shorter-than-Gaussian high-side temperature distribution tails over NA and documents the effect on extreme warm temperature exceedances under a simple uniform warm shift in the distribution. This shift may also be interpreted as a measure of the departure from Gaussianity, with associated statistical significance estimates. Locations exhibiting short warm tails experience a larger increase in the fraction of days exceeding the current P95 of the distribution under this shift, suggesting that these locations may be more prone to large changes in heat extremes. It is notable that examples were found throughout the domain from the Arctic to the tropics. Areas exhibiting particularly large increases in extreme warm exceedances are along the northern Pacific coast and along the U.S./Canada border from the Rocky Mountains to the Great Plains and the Gulf of Mexico coast in winter. In summer, high-side tails deviate less dramatically from Gaussian, but northern Alaska and western Canada, the western and eastern U.S., and the Gulf of Mexico coast show relatively large increases in warm threshold exceedances with the shift in the distribution.

These results have significant implications for future climate impacts from extreme warm temperatures in regions identified as having shorter-than-Gaussian high-side tails. If global warming is largely manifested as a shift in the mean, the shift measure used here can be directly interpreted in terms of the more rapid than Gaussian increase of the exceedances. While the majority of evidence suggests warming is likely to be largely realized as a change in the mean in most regions, some locations may respond differently, especially in places where large excursions on the warm side of the PDF may currently be limited by adjacent bodies of water, disappearing snow and ice cover (such as in Figure 2d), or where changes in atmospheric circulation could affect the distribution tails. In this case, the short tails are indications of dynamical processes that affect the distribution in ways more complex than the two parameters of a Gaussian. Changes in other moments of the distribution may also play a role, such as decreasing variance over time [*Schneider et al*., 2015]. While this paper focuses on short warm tails, the effect of shorter-than-Gaussian cold tails would be associated with large decreases in extreme cold exceedances. Such cases could be associated with additional impacts such as large reductions in days falling below freezing with implications for snow and ice cover reductions and potential biological impacts. All cases imply that climate models must be able to realistically reproduce temperature distribution tails as a first step to reliably projecting future changes in temperature extremes.

Acknowledgments

Part of this research was carried out at the Jet Propulsion Laboratory, California Institute of Technology, under a contract with the National Aeronautics and Space Administration, and part was funded by NSF AGS-1102838/AGS-1540518, NOAA NA14OAR4310274 (J.D.N.), and NASA NCA 11-NCA11-0028 (P.C.L.). Temperature data were obtained at 10.5065/D6PR7SZF. We thank Joyce Meyerson for computational and graphical assistance.

The Editor thanks two anonymous reviewers for their assistance in evaluating this paper.

References

Bourlioux, A., and A. J. Majda (2002), Elementary models with probability distribution function intermittency for passive scalars with a mean gradient, *Phys. Fluids*, *14*, 881–897.

Cavanaugh, N. R., and S. S. P. Shen (2014), Northern Hemisphere climatology and trends of statistical moments documented from GHCN-daily surface air temperature station data from 1950 to 2010, *J. Clim.*, *27*, 5396–5410.

Christidis, N. (2005), Detection of changes in temperature extremes during the second half of the 20th century, *Geophys. Res. Lett.*, *32* L20716, doi:10.1029/2005GL023885.

Coumou, D., and A. Robinson (2013), Historic and future increase in the global land area affected by monthly heat extremes, *Environ. Res. Lett.*, *8*, doi:doi:10.1088/1748-9326/8/3/034018.

Donat, M. G., and L. V. Alexander (2012), The shifting probability distribution of global daytime and night-time temperatures, *Geophys. Res. Lett.*, *39*, L14707, doi:10.1029/2012GL052459.

Donat, M. G., et al. (2013), Updated analyses of temperature and precipitation extreme indices since the beginning of the twentieth century: The HadEX2 dataset, *J. Geophys. Res. Atmos.*, *118*, 2098–2118, doi:10.1002/jgrd.50150.

Fischer, E. M., and R. Knutti (2014), Detection of spatially aggregated changes in temperature and precipitation extremes, *Geophys. Res. Lett.*, *41*, 547–554, doi:10.1002/2013GL058499.

Huntingford, C., P. D. Jones, V. N. Livina, T. M. Lenton, and P. M. Cox (2013), No increase in global temperature variability despite changing regional patterns, *Nature*, *500*, 327–330.

Huybers, P., K. A. McKinnon, A. Rhines, and M. Tingley (2014), U.S. daily temperatures: The meaning of extremes in the context of non-normality, *J. Clim.*, *27*, 7368–7384.

Kharin, V. V., F. W. Zwiers, X. Zhang, and G. C. Hegerl (2007), Changes in temperature and precipitation extremes in the IPCC ensemble of global coupled model simulations, *J. Clim.*, *20*, 1419–1444.

Kharin, V. V., F. W. Zwiers, X. Zhang, and M. Wehner (2013), Changes in temperature and precipitation extremes in the CMIP5 ensemble, *Clim. Change*, *119*, 345–357, doi:10.1007/s10584-013-0705-8.

Kirtman, B., et al. (2013), Near-term climate change: Projections and predictability, in *Climate Change 2013: The Physical Science Basis. Contribution of the Working Group I to the Fifth Assessment Report of the Intergovernmental Panel on Climate Change*, edited by T. F. Stokcer et al., pp. 953–1028, Cambridge Univ. Press, Cambridge, U. K., and New York.

Lau, N.-C., and M. J. Nath (2012), A model study of heat waves over North America: Meteorological aspects and projections for the twenty-first century, *J. Clim.*, *25*, 4761–4784.

Loikith, P. C., and A. J. Broccoli (2012), Characteristics of observed atmospheric circulation patterns associated with temperature extremes over North America, *J. Clim.*, *25*, 7266–7281.

Loikith, P. C., B. R. Lintner, J. Kim, H. Lee, J. D. Neelin, and D. E. Waliser (2013), Classifying reanalysis surface temperature probability density functions (PDFs) over North America with cluster analysis, *Geophys. Res. Lett.*, *40*, 3710–3714, doi:10.1002/grl.50688.

Loikith, P. C., D. Waliser, H. Lee, J. D. Neelin, B. R. Lintner, S. McGinnis, L. O. Mearns, and J. Kim (2015a), Evaluation of large-scale meteorological patterns associated with temperature extremes in the NARCCAP regional climate model simulations, *Clim. Dyn.*, doi:10.1007/s00382-015-2537-x.

Loikith, P. C., D. E. Waliser, H. Lee, J. Kim, J. D. Neelin, B. R. Lintner, S. McGinnis, C. Mattmann, and L. O. Mearns (2015b), Surface temperature probability distributions in the NARCCAP hindcast experiments: Evaluation methodology, metrics and results, *J. Clim.*, *28*, 978–997.

Majda, A. J., and B. Gershgorin (2010), Quantifying uncertainty in climate change science through empirical information theory, *Proc. Natl. Acad. Sci. U.S.A.*, *107*, 14,958–14,963.

Meehl, G. A., C. Tebaldi, G. Walton, D. Easterling, and L. McDaniel (2009), Relative increase of record high maximum temperatures compared to record low minimum temperatures in the U.S, *Geophys. Res. Lett.*, *36*, L23701, doi:10.1029/2009GL040736.

Mitchell, T. D., and P. D. Jones (2005), An improved method of constructing a database of monthly climate observations and associated high-resolution grids, *Int. J. Climatol.*, *25*, 693–712.

Morak, S., G. C. Hegerl, and N. Christidis (2013), Detectable changes in the frequency of temperature extremes, *J. Clim.*, *26*, 1561–1574.

Neelin, J. D., B. R. Lintner, B. Tian, Q. Li, L. Zhang, P. K. Patra, M. T. Chahine, and S. N. Stechmann (2010), Long tails in deep columns of natural and anthropogenic tropospheric tracers, *Geophys. Res. Lett.*, *37*, L05804, doi:10.1029/2009GL041726.

Perkins, S. E., L. V. Alexander, and J. R. Nairn (2012), Increasing frequency, intensity and duration of observed global heatwaves and warm spells, *Geophys. Res. Lett.*, *39*, L20714, doi:10.1029/2012GL053361.

Perron, M., and P. Sura (2013), Climatology of non-Gaussian atmospheric statistics, *J. Clim.*, *26*(3), 1063–1083.

Rhines, A., and P. Huybers (2013), Frequent summer temperature extremes reflect changes in the mean, not the variance, *Proc. Natl. Acad. Sci. U.S.A.*, *110*, E546, doi:10.1073/pnas.1218748110.

Rienecker, M. M., et al. (2011), MERRA: NASA's Modern-Era Retrospective Analysis for Research and Applications, *J. Clim.*, *24*, 3624–3648.

Rowe, C. M., and L. E. Derry (2012), Trends in record-breaking temperatures for the conterminous United States, *Geophys. Res. Lett.*, *39*, L16703, doi:10.1029/2012GL052775.

Ruff, T. W., and J. D. Neelin (2012), Long tails in regional surface temperature probability distributions with implications for extremes under global warming, *Geophys. Res. Lett.*, *39*, L04704, doi:10.1029/2011GL050610.

Schneider, T., T. Bischoff, and H. Płotka (2015), Physics of changes in synoptic midlatitude temperature variability, *J. Clim.*, *28*, 2312–2331.

Seneviratne, S. I., et al. (2012), Changes in climate extremes and their impacts on the natural physical environment, in *Managing the Risks of Extreme Events and Disasters to Advance Climate Change Adaptation. A Special Report of Working Groups I and II of the Intergovernmental Panel on Climate Change (IPCC)*, edited by C. B. Field, pp. 109–230, Cambridge Univ. Press, Cambridge, U. K., and New York.

Sheskin, D. (2003), *Handbook of Parametric and Nonparametric Statistical Procedures*, 3rd ed., Chapman & Hall/CRC, Boca Raton, Fla.

Sillmann, J., V. V. Kharin, X. Zhang, F. W. Zwiers, and D. Bronaugh (2013), Climate extremes indices in the CMIP5 multimodel ensemble: Part 1. Model evaluation in the present climate, *J. Geophys. Res. Atmos*, *118*, 1716–1733, doi:10.1002/jgrd.50203.

Stefanova, L., P. Sura, and M. Griffin (2013), Quantifying the non-Gaussianity of wintertime daily maximum and minimum temperatures in the southeast, *J. Clim.*, *26*, 838–850.

Wang, A., and X. Zeng (2013), Development of global hourly 0.5° land surface air temperature datasets, *J. Clim.*, *26*, 7676–7691.

Wang, A., and X. Zeng (2014a), *Global Hourly 0.5-Degree Land Surface Air Temperature Datasets*, Research Data Archive at the National Center for Atmospheric Research, Computational and Information Systems Laboratory, Boulder, Colo., doi:10.5065/D6PR7SZF.

Wang, A., and X. Zeng (2014b), Range of monthly mean hourly land surface air temperature diurnal cycle over high northern latitudes, *J. Geophys. Res. Atmos.*, *119*, 5836–5844, doi:10.1002/2014JD021602.

Wang, A., and X. Zeng (2015), Global hourly land surface air temperature datasets: Inter-comparison and climate change, *Int. J. Climatol.*, doi:10.1002/joc.4257.

Weaver, S. J., A. Kumar, and M. Chen (2014), Recent increases in extreme temperature occurrence over land, *Geophys. Res. Lett.*, *41*, 4669–4675, doi:10.1002/2014GL060300.

Zwiers, F. W., X. Zhang, and Y. Feng (2011), Anthropogenic influence on long return period daily temperature extremes at regional scales, *J. Clim.*, *24*, 881–892.